CHEMISTRY
A EUROPEAN JOURNAL

DOI: 10.1002/chem.200601276

Electrochemical, Pulsed-Field-Gradient Spin-Echo NMR Spectroscopic, and ESR Spectroscopic Study of the Diffusivity of Molecular Probes inside Gel-Type Cross-Linked Polymers

Benedetto Corain,*[a] Angelo A. D'Archivio,*[b] Luciano Galantini,[c] Silvano Lora,[d] Abdirisak A. Isse,[a] and Flavio Maran*[a]

Abstract: The permeability of five gel-type synthetic resins, obtained by polymerization of 1-vinylpyrrolidin-2-one cross-linked with *N*,*N*′-methylenebisacrylamide (1, 2, 3, 4, and 5 wt%) and swollen by *N*,*N*-dimethylformamide (DMF), has been analyzed. The diffusion of 2,2,6,6-tetramethyl-4-oxo-1-piperidinyloxyl (TEMPONE) was studied by ultramicroelectrode voltammetry. Similar measurements were performed for solutions of non-cross-linked poly(vinylpyrrolidone) in DMF. To provide information on the rotational mobility of TEMPONE and the translational mobility of DMF, electron spin resonance (ESR) spectroscopic and pulsed-field-gradient spin-echo nuclear magnetic resonance (PGSE-NMR) spectroscopic experiments, respectively, were carried out. Comparative analysis of the results obtained by electrochemical, ESR spectroscopic, and PGSE-NMR spectroscopic measurements showed that diffusivity inside the polymer framework is significantly affected by the extent of cross-linking, the size of the diffusing probe, and the presence of electrolytes.

Keywords: diffusion · electrochemistry · gels · polymers

Introduction

Cross-linked functional polymers (CFPs), also known as functional resins, are cross-linked macromolecular organic materials built up of covalently interconnected chains in which the cross-links are formed by using polyfunctional vinyl co-monomers in the polymerization reaction.[1] Gel-type CFPs are economically important materials that are successfully employed as ion exchangers,[2] solid strong acids,[3] and "solid phase" reagents in synthetic organic chemistry.[4] CFPs have long been considered[5] useful supports for metal catalysis (hybrid-phase metal catalysis),[6] the main goal being to employ catalytically active metal coordination compounds, chemically connected to polymer frameworks, in chemical processing.[7] In this connection, it is worth mentioning that after decades of unsatisfied expectation[7,8] an important industrial process for the production of acetic acid, based on the use of a Ⓟ$^{+}[Rh(CO)_2I_2]^{-}$ ion pair (see below) (Ⓟ = polymer; in particular, partially iodomethylated poly(4-vinylpyridine)), could be eventually developed in the late nineties.[9] In addition to the strategy of supporting molecularly defined and catalytically active coordination compounds, CFPs are currently viewed[10,11] as promising supports for nanoclustered metals, mostly palladium and gold, to be employed as catalysts in chemical processing. For both Ⓟ-[L′-ML_n] and Ⓟ/M^0 catalytic systems, the issues of characterizing and understanding the nanomorphology and molecular accessibility of the polymer framework play a crucial role in assessing catalyst activity and in devising possible process technologies.

During the last decade we focused on the synthesis and physicochemical characterization of Ⓟ/M^0 catalysts and of promising CFPs. Significant achievements range from the

[a] Prof. B. Corain, Dr. A. A. Isse, Prof. F. Maran
Dipartimento di Scienze Chimiche, Università di Padova
Via Marzolo 1, 35131 Padova (Italy)
Fax (+39) 049-827-5239
E-mail: benedetto.corain@unipd.it
flavio.maran@unipd.it

[b] Prof. A. A. D'Archivio
Dipartimento di Chimica Ingegneria Chimica e Materiali
Università di L'Aquila
Via Vetoio Coppito 2, 67010 L'Aquila (Italy)
Fax: (+39) 0862-433753
E-mail: darchivi@univaq.it

[c] Dr. L. Galantini
Dipartimento di Chimica, Università di Roma "La Sapienza"
P.zale Aldo Moro 5, 00185 Roma (Italy)

[d] Dr. S. Lora
Istituto per la Sintesi Organica e la Fotoreattività, C.N.R.
Via Romea 4, 35020 Legnaro, Padova (Italy)

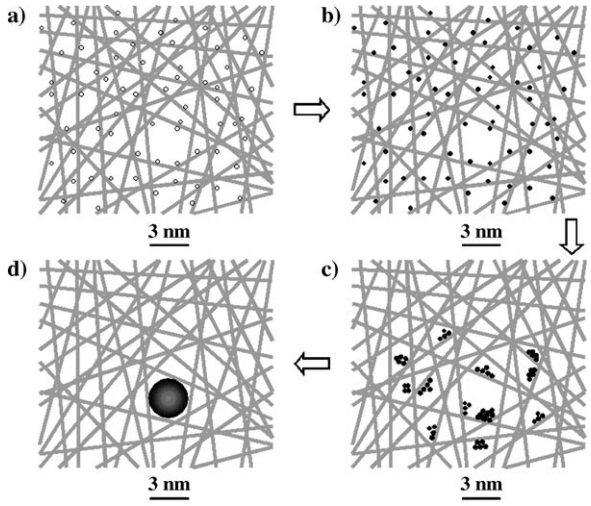

Figure 1. Description of the polymer network of a cross-linked functional polymer in the swollen state according to Ogston's model[46] and the model for the generation of size-controlled metal nanoparticles inside metalated CFPs. a) Pd^{II} is homogeneously dispersed inside the polymer framework; b) Pd^{II} is reduced to Pd^0; c) Pd^0 atoms start to aggregate; d) a single $\approx$3 nm nanocluster is formed and trapped inside of the largest mesh present in that volume of the polymer framework. This figure is taken from ref. [10b].

production of resin-supported size-controlled Pd^0 and Au^0 nanoclusters (Figure 1)[10a,b] to a detailed description of typical CFP frameworks, taking advantage of substantial information obtained from various physicochemical tools such as inverse steric exclusion chromatography (ISEC),[12] electron spin resonance (ESR) spectroscopy,[12b] pulsed-field-gradient spin-echo NMR (PGSE-NMR) spectroscopy,[13] and cross-polarization magic angle spinning (CP MAS) ^{13}C NMR spectroscopy.[14] These techniques are particularly useful for investigating what the interior of swollen resin particles could look like.[12,13] Gel-type CFPs are unconventional media that may be viewed as solutions of interconnected polymer chains that produce a porous medium allowing diffusion of properly sized solutes. From an applied point of view, this aspect is related to the problem of understanding how these resin particles may behave while in a fixed-bed or a slurry reactor, as each particle may be considered as a microreactor. Thus, reagents involved in a given metal-catalyzed reaction must be able to enter the microreactor (size selectivity) where they will experience a medium (e.g., a mixture of two different solvents) the composition of which could be quite different from that of the bulk of the reaction medium. Consequently, the kinetics and thermodynamics of the catalyzed reaction might differ significantly from those typical of the bulk,[15] and so could the reagents' activities. Because of these and other features, metal catalysts based on functional resins are emerging as innovative catalysts in which the polymeric support is able to exert promotion or co-catalytic actions that would be inconceivable for conventional metal catalysts based on metal oxides or amorphous carbon.[16]

In this paper we describe the results of an investigation aimed at characterizing the diffusivity inside a series of ad hoc synthesized CFPs. The gel-type CFPs were prepared from 1-vinylpyrrolidin-2-one cross-linked by copolymerization with *N*,*N*′-methylenebisacrylamide and then swollen by *N*,*N*-dimethylformamide (DMF). These CFPs were characterized by moderate cross-linking degrees (1, 2, 3, 4 and 5 wt%, **M1**, **M2**, **M3**, **M4** and **M5**, respectively) and designed to possess average polymer-chain concentrations ranging from about 0.2 to 2.0 nm^{-2} in polar solvents, which corresponds to nanometer-sized pores.[12a] To better appreciate the cross-linking effects, solutions of the non-cross-linked poly(vinylpyrrolidone) (PVP) in DMF were also investigated. The study was carried out by using ESR spectroscopy, PGSE-NMR spectroscopy, and ultramicroelectrode cyclic voltammetry (CV). We determined both the translational and rotational mobility of 2,2,6,6-tetramethyl-4-oxo-1-piperidinyloxyl (TEMPONE), which is both a convenient redox agent and spin probe. Whereas the rotational mobility of TEMPONE was studied by ESR spectroscopy, the diffusion of TEMPONE was analyzed by CV using a double-shield platinum ultramicrodisk electrode.[17] In fact, electrochemical techniques employing ultramicroelectrodes have been successfully employed to measure the behavior of electroactive species dissolved in different conductive frameworks such as polyelectrolytes,[18] latex suspensions,[19] and sol–gel silica matrices.[20] Further insights into the translational dynamics in the swollen CFPs were obtained from PGSE-NMR spectroscopic measurements of the diffusion of the DMF solvent itself. To obtain complementary information on the investigated systems, we studied the diffusion of the probes at different temperatures. The results obtained by these independent and complementary techniques showed how and to what extent the mobility of molecules is reduced when these species are confined in the supramolecular cages provided by swollen CFPs.

Experimental Section

Materials: 1-Vinylpyrrolidin-2-one (Acros), *N*,*N*′-methylenebisacrylamide (Sigma Aldrich), and poly(vinylpyrrolidone) (Sigma Aldrich, MW 29000) were used as received. 2,2,6,6-Tetramethyl-4-oxo-1-piperidinyloxyl (Sigma) was recrystallized from *n*-hexane. *N*,*N*-Dimethylformamide (Acros, 99%) was treated for a few days with anhydrous Na_2CO_3, whilst stirring, and then distilled at reduced pressure under nitrogen. The solvent was collected in dark bottles and stored under nitrogen. The supporting electrolyte was tetraethylammonium perchlorate (TEAP, Fluka 99%) which was recrystallized twice from ethanol and dried at 60°C under vacuum.

The CFPs were synthesized at room temperature by exposure of the appropriate mixture of the two co-monomers, 1-vinylpyrrolidin-2-one and *N*,*N*′-methylenebisacrylamide, to a γ-ray ^{60}Co source for 18 h. The dose rate was 0.154 $Gy\,s^{-1}$ (total dose: 10 KGy) leading to 100% polymerization. The CFPs were labeled as **M1, M2**, **M3**, **M4**, and **M5** according to the weight percentage of the cross-linker in the mixture. The CFPs, obtained as cylindrical pale-yellow glassy rods (40 mm length, 10 mm diameter), were cut to 2 mm thick slices and used as such for the electrochemical measurements. Smaller fragments were used in the ESR and PGSE-NMR spectroscopy experiments.

Electrochemical apparatus and procedures: The electrochemical instrumentation employed in the cyclic voltammetry experiments was a PC-controlled EG&G-PARC 273A potentiostat–galvanostat. A three-electrode configuration system was employed. A 0.5 mm diameter silver wire was used as a quasireference electrode (AgQRE) and the working electrode was a 11.1 μm radius platinum ultramicrodisk electrode, which was built starting from a platinum microwire (Goodfellow, Cambridge, UK) having a nominal radius of 10 μm. The actual radius was calculated by studying the oxidation of ferrocene, whose diffusion coefficient is 1.13×10^{-5} cm^2s^{-1} in DMF/0.1 M TEAP.[21] The radius proved to be constant in all the experiments. The ultramicrodisk electrode was prepared according to a special procedure devised to provide low-noise electrodes thanks to an efficient electrical double shield.[17] Before each measurement, the electrode was polished with a 0.25 μm diamond paste (Struers) and then rinsed ultrasonically with ethanol for 5 min. Electrochemical activation of the electrode, carried out by cycling its potential over a wide range in the background solution, did not significantly improve the quality and reproducibility of the experimental results.

To carry out the electrochemical measurements, a simple but efficient electrochemical apparatus was built. A small (5 mL) conical glass cell was equipped with a Teflon cap and, at the bottom, with a 10 mm diameter glass frit. The glass frit served to evacuate, when required, the solution from the cell; this operation was carried out by releasing an underneath valve and by applying a positive argon pressure inside the cell. The Teflon cap held the three electrodes and a series of Teflon tubes; these tubes served as the inlet/outlet of the purging gas (argon) and to introduce, from external containers, either the background solution (DMF containing 0.2 or 0.6 M TEAP) or a 10^{-2} M TEMPONE solution in the same solvent/electrolyte system. By applying an argon pressure inside the appropriate container, the cell could be easily filled. A resin disk was positioned at the bottom of the cell and then covered and swollen with the DMF solution for 3–4 h. The double-shield platinum working electrode was positioned at variable distances with respect to the swollen CFP. The counter electrode, which was a 6 mm diameter platinum disk, was positioned at the bottom of the cell between the polymer sample and the glass frit. By vertically adjusting the position of the working electrode, it was possible to carry out the CV experiment either in the supernatant electrolyte solution or in the underlying swollen polymer network. In the latter case, the electrode was gently forced into the swollen resin. CV curves for the oxidation of TEMPONE were recorded at scan rates in the range of 0.02–0.4 $V s^{-1}$, first in the bulk DMF solution and then in the swollen polymer. To ensure reproducibility, the procedure was repeated at least three times. All measurements were carried out at room temperature (22 ± 1 °C).

Electron spin resonance spectroscopy: Small fragments of dry CFP were swollen with a nitrogen-saturated 10^{-4} M DMF solution of the paramagnetic probe TEMPONE. After reaching the swelling equilibrium, the excess solution was removed by swiping the particle with filter paper and a suitable amount of swollen CFP was quickly transferred into the ESR spectroscopy tube. The spectra were recorded in the temperature range of 5–35 °C, at intervals of 5 °C, using an X-band JEOL JES-RE1X apparatus working at 9.2 GHz (modulation 100 kHz). During the measurements, the temperature of the sample was controlled (±0.1 °C) using a variable-temperature unit (Steler VTC91).

The spectra obtained were typical of a fast-motion regime.[22] Hence, the rotational correlation time τ of TEMPONE was calculated according to the Equation (1),[23] where $\omega_e = 5.78\times10^{10}$ Hz. The parameters h_{+1}, h_0, and h_{-1} (intensities of the low-, middle-, and high-field lines, respectively) and ΔH_0 (peak-to-peak width of the central line, in G) were obtained by peak-picking from the first-derivative spectrum. The numerical constant (in sG^{-1}) was evaluated by using known values of the anisotropic g factor and the hyperfine tensors of TEMPONE.[24]

$$\tau = 6.14\times10^{-10}\,\Delta H_0\left[\left(\frac{h_0}{h_{+1}}\right)^{1/2}+\left(\frac{h_0}{h_{-1}}\right)^{1/2}-2\right][1-{}^1/_5(1+\omega_e^2\tau^2)] \quad (1)$$

Pulsed-field-gradient spin-echo NMR spectroscopy: The self-diffusion coefficient of DMF was determined by ^{1}H PGSE-NMR spectroscopy. In this technique,[25] a spin-echo experiment is performed while two magnetic-field-gradient pulses of magnitude G, duration δ, and separation Δ are applied during the dephasing and rephasing periods. The interval Δ between the magnetic-field-gradient pulses was kept constant and equal to the interval t between the 90–180° radio frequency pulses. Under these conditions, for a "nucleus" with diffusion coefficient D, the height of the echo amplitude A is given by Equation (2), where γ is the magnetogyric ratio and T_2 is the spin–spin relaxation time of the nucleus. In a typical experiment, A was measured at $\Delta = 20$ ms and $G = 14.4$ $G cm^{-1}$, varying δ up to 15 ms. The gradient strength was calibrated against values of the self-diffusion coefficient of pure water. Because of the relatively short T_2 relaxation time of the polymer's hydrogen atoms, the selected t value was sufficient to remove the polymer contribution from the echo signal. The solvent diffusion coefficient was obtained from the slope of the logarithmic plot of A versus $\delta^2(\Delta-\delta/3)$. The samples were prepared as described above for the ESR spectroscopy experiments and placed in a 5 mm NMR spectroscopy tube. The spectra were recorded on a Bruker SXP 4–100 MHz apparatus operating at 21 MHz for protons over the temperature range of 10–35 °C, at intervals of 5 °C. During the measurements, the temperature of the sample was controlled (±0.25 °C) using a variable-temperature unit (Bruker-VT 100).

$$A = A_0\exp\left[\frac{-2t}{T_2}-\gamma^2G^2D\delta^2\left(\Delta-\frac{\delta}{3}\right)\right] \quad (2)$$

Results and Discussion

Swelling behavior: The CFPs **M1**–**M5** swelled appreciably in DMF. The swelling data, displayed as the ratio R between the solvent volume and the dry polymer mass, are collected in Table 1. As expected, the extent of swelling decreased as the cross-linking degree increased. The presence of 0.6 M TEAP, the electrolyte used in the CV measurements, had no significant effect. Table 1 also shows the polymer mass concentration (w, in terms of weight percentage, wt %) and the polymer volume fraction (φ), which was calculated from w using Equation (3), where d_{PVP} and d_{DMF} are the densities of PVP (assumed to be the same as that of the cross-linked polymer forming **M1**–**M5**) and DMF, respectively. All calculations were carried out using $d_{PVP} = 1.275$ $g mL^{-1}$[26] and $d_{DMF} = 0.944$ and 0.959 $g mL^{-1}$ for pure DMF and DMF/0.6 M TEAP, respectively, assuming additivity of the partial volumes of PVP and DMF (or DMF/0.6 M TEAP).

Table 1. Swelling behavior of CFPs **M1–M5** in DMF and DMF/0.6 M TEAP.

CFP	wt %[a]		R [mL g^{-1}][a]		φ[a]	
M1	19.0	18.0	4.52	4.74	0.15	0.14
M2	28.2	31.9	2.70	2.23	0.23	0.26
M3	30.9	33.4	2.37	2.08	0.25	0.27
M4	38.7	39.9	1.68	1.57	0.32	0.33
M5	52.5	53.1	0.96	0.92	0.45	0.46

[a] The second figure refers to experiments in DMF/0.6 M TEAP.

$$\varphi = \frac{(w/d_{PVP})}{\{[(100-w)/d_{DMF}]+(w/d_{PVP})\}} \quad (3)$$

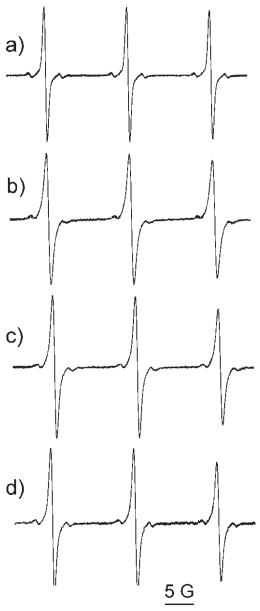

Figure 2. ESR spectra of TEMPONE in a) DMF and in DMF-swollen b) **M1**, c) **M3**, and d) **M5** at $T=25\,^{\circ}C$.

ESR and PGSE-NMR spectroscopic measurements: ESR spectroscopic measurements were carried out on CFPs **M1**–**M5** swollen by either DMF or DMF/0.6 M TEAP. The data were collected in the temperature range of 5–30 °C. In all cases, the ESR spectra of TEMPONE exhibited a relatively narrow triplet (Figure 2), as expected for a nitroxide radical in a fast rotational regime (rotational correlation time $\tau = 10^{-11}$–10^{-9} s). The τ values (Table 2) were calculated from the ESR spectroscopic line widths of these spectra, as explained in the Experimental Section. The isotropic ^{14}N hyperfine coupling constant, which is a good indicator of solvent polarity[27] and is defined as one half of the separation between the $+1$ and -1 spectral lines, was independent of the parameter φ. This finding suggests that the interactions between the spin probe and the polymer chains are negligible. Therefore, the τ values should be viewed as reflecting purely microviscosity effects. When passing from the bulk solvent to the solvent confined inside the gel-type polymer network, the decrease of the rotational mobility of TEMPONE was apparent with both DMF and DMF/0.6 M TEAP as swelling agents. Table 2 shows that the increase in polymer-chain concentration caused by an increase in cross-linking (polymer volume fraction) is indeed matched by an increase of τ (reduced mobility). The rotational mobility of TEMPONE was also affected by the nature of the swelling medium, as the τ values were always a little larger in the presence of the supporting electrolyte; this is in keeping with an appreciable increase in the viscosity of the medium (see later).

Table 2. Rotational correlation time of TEMPONE and self-diffusion coefficient of DMF at 25 °C and relevant activation energies.

Medium	TEMPONE				DMF		
	$\tau(\pm5\,\%)^{[a,b]}$ [ps]		$E_a^{[a,b,c]}$ [kJ mol^{-1}]		$D(\pm5\,\%)^{[a,d]}$ [10^{-7}cm^{2}s^{-1}]		$E_a^{[c]}$ [kJ mol^{-1}]
bulk solution	13	14	9(1)	11(1)	163	112	9(1)
M1	21	24	9(1)	12(1)	120		11(1)
M2	25	30	9(1)	15(1)	86	66	10(1)
M3	31	34	10(1)	17(2)	63		13(1)
M4	37	41	13(1)	19(2)	52		13(1)
M5	37	40	12(1)	21(2)	52		13(1)

[a] The first figure refers to DMF. [b] The second figure refers to DMF/0.6 M TEAP. [c] The uncertainty is given in parentheses. [d] The second figure refers to DMF/0.6 M $LiClO_4$.

The PGSE-NMR spectroscopic measurements were recorded in the temperature range of 10–35 °C after allowing the CFPs to swell with DMF. As for the ESR spectroscopy results, the PGSE-NMR spectroscopic measurements revealed a similar correlation (Table 2) between the decrease of the diffusion coefficient D of DMF and the increase of the cross-linking degree. The presence of 0.6 M $LiClO_4$ reduced the diffusion coefficient of DMF appreciably.

In terms of rotational mobility and self-diffusion no clear difference between **M4** and **M5** could be detected. On the other hand, from previous chromatographic studies (ISEC)[12–14] we have learned that in a series of related CFPs an increase of the polymer volume fraction is accompanied by a concomitant increase of regions of the swollen CFP that are inaccessible even to the smallest molecular probes employed in the ISEC measurements. This implies that the higher percentage of cross-linking in **M5** may lead to a swollen polymer framework in which a higher percentage of gel mass lacks any perceivable porosity but the remaining gel mass is comparatively accessible to diffusing molecules in both **M4** and **M5**. This would lead to similar τ and D values inside these two CFPs.

Temperature studies: A first-level evaluation of diffusivity inside polymer networks can be achieved by studying the effect of temperature on the rotational and translational mobilities of confined molecular probes.[28,29] For CFPs **M1**–**M5**, the plots of $\ln\tau$ and $\ln D_{DMF}$ versus $1/T$ were satisfactorily linear (r^2 values in the ranges of 0.967–0.995 and 0.965–0.978 for the ESR and NMR spectroscopy plots, respectively) in the temperature range explored. The corresponding Arrhenius activation energies (E_a) are collected in Table 2. It is worth noting that the E_a values obtained from ESR and NMR spectroscopic measurements in DMF are essentially coincident with the value of 9.7 kJ mol^{-1} that can be calculated from literature data on the dependence of the viscosity η of DMF on T in the temperature range of 20–80 °C.[30] Therefore, our results agree with the behavior expected for viscosity-controlled processes.

No effect of the polymer network on E_a was observed for the rotational mobility of TEMPONE in the DMF-swollen resins **M1** and **M2**, while a slight increase was detected for rotational mobility in **M3**–**M5**. Noteworthy, when the resins were swollen by DMF/0.6 M TEAP the E_a values increased steadily and markedly on going from the pure electrolyte solution to swollen **M5**. For the diffusion of DMF, a slight increase of E_a was observed on going from pure DMF to **M3**, but for samples with higher degrees of cross-linking no further increase was detectable beyond the bounds of experimental error. Overall, E_a is thus mildly dependent on the polymer volume fraction φ, and TEMPONE and DMF appear to be mobile in media in which the major role of the polymer network is to generate an uncomplicated cavity effect typical of motions inside nanoporous[31] domains of low density. That the motions in these CFPs are viscosity-controlled processes is also supported by the data obtained in the presence of an electrolyte, which increases the

medium viscosity and makes molecular motions more sensitive toward temperature changes.

Cyclic voltammetry: Ultramicroelectrodes (UMEs)[32] are electrodes in which at least one dimension does not exceed 20–30 μm. A consequence of the size effect is that the electrochemical behavior may be either the same or substantially different from that of conventional millimeter-sized electrodes. The actual outcome is a function of the timescale of the CV experiment, which can be modulated by varying the potential scan rate (v). Let us now focus on CV at ultramicrodisk electrodes. When the timescale of the experiment is short enough (high v values), the thickness of the diffusion layer is small compared to the radius of the electrode and thus the voltammetric curve is peak-shaped, as observed with larger electrodes, because semi-infinite linear diffusion conditions are attained. On the other hand, when the timescale is sufficiently long (low v values), the thickness of the diffusion layer becomes much larger than the electrode radius r, leading to an efficient radial diffusion regime; the curve now has a sigmoidal shape and the backward scan reproduces the trace of the forward scan. It is useful to introduce the dimensionless parameter $(Dt)^{1/2}/r$, where t is the microelectrolysis time and the numerator describes the thickness of the diffusion layer. Thus, when $(Dt)^{1/2}/r \gg 1$, the system is under radial steady-state diffusion and the limiting current of the voltammetric plateau (i_l) is independent of v and directly proportional to both D and r [Eq. (4),[32] where n is the number of electrons exchanged in the electrode process, F is the Faraday constant, and C is the bulk concentration of the electroactive species]. On the other hand, linear diffusion prevails for $(Dt)^{1/2}/r \ll 1$ and the maximum current for a reversible process, which now is the peak current (i_p), becomes proportional to $v^{1/2}$, $D^{1/2}$, and the electrode area A [Eq. (5)].

$$i_l = 4nFDCr \tag{4}$$

$$i_p = 0.4463nFAC\left(\frac{nFvD}{RT}\right)^{1/2} \tag{5}$$

For intermediate values of $(Dt)^{1/2}/r$, mixed diffusion conditions are attained. Therefore, because of a different D dependence, low scan rate measurements at ultramicrodisk electrodes are particularly sensitive in determining D values. This is also true when the goal is to determine the decrease of D caused by an increase of the viscosity η of the medium, which can be related to D through the Stokes–Einstein equation [Eq. (6), where k_B is the Boltzmann constant]. For any given combination of v and r values, a decrease of D causes a transition from radial to linear diffusion conditions, which leads to a reduced sensitivity. Generally speaking, this also implies that the ideal conditions for performing diffusivity measurements may differ slightly when the viscosity of the medium is varied.

$$D = \frac{k_B T}{6\pi\eta r} \tag{6}$$

Figure 3 shows CV curves for the oxidation of TEMPONE in DMF/0.6 M TEAP and after making contact between the electrode and some of the swollen CFPs. The

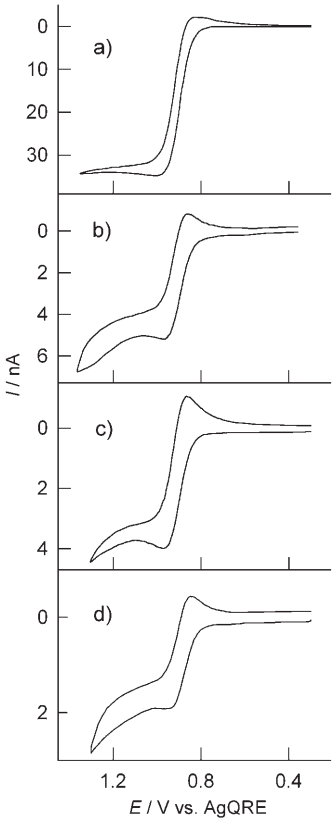

Figure 3. Cyclic voltammograms for the oxidation of 11 mM TEMPONE in a) DMF and in DMF-swollen b) **M2**, c) **M3**, and d) **M5**. Conditions: 11.1 μm radius Pt electrode, 0.6 M TEAP, $v = 0.1$ V s^{-1}, $T = 22$ °C.

electrode reaction is the reversible one-electron oxidation of the nitroxide radical to the oxoammonium ion. The current increase observed at the most positive potentials was caused by impurities trapped during the formation of the polymer. In fact, all polymers were originally formed as pale-yellow glassy solids. However, by allowing the CFPs to be swollen by the DMF solution for a few hours, draining the solution from the cell, refilling it with fresh solution, and by repeating the procedure a couple of times, we noticed that almost transparent samples could be obtained and the current increase before reversal of the potential scan was essentially absent. Although this long pretreatment did not affect either the maximum current or the shape of the actual oxidation wave, it eventually resulted in a less homogeneous gel, probably because of some cracking–softening process. Consequently, all measurements were carried out only on freshly cut CFP samples that were allowed to equilibrate with the TEMPONE-containing solution for 3–4 h.

The voltammetric pattern illustrated in Figure 3 shows that on going from bulk DMF to the swollen polymers a considerable decrease of the voltammetric current took place. At the same time, the shape of the CV curve gradually changed from the almost sigmoidal shape observed in the bulk solution (curve a) to the peak-shaped reversible CV curves in the swollen CFPs. The observed changes in the voltammetric pattern pointed to a significant decrease of the diffusion rate as the medium changed from a free to a confined solvent. Although at first sight the current decrease could be attributed to a decrease of the active electrode surface, the shape change provided compelling evidence for a concomitant change in the diffusional regime. As described above, this change can only be ascribed to a reduced value of the average diffusion coefficient (but not to a decrease of the electrode area and thus of the effective radius). We can thus conclude that diffusion is indeed significantly hampered by the extent of cross-linking in the polymer network.

Our data pointed to mixed diffusion conditions and could be conveniently treated by expressing the maximum current according to Equation (7) derived by Aoki et al.,[33] where $p=(nFvr^2/RTD)^{1/2}$. In each experiment, series of voltammograms were recorded in the bulk solution and in the swollen CFP. Equation (7) was used to calculate the D value of TEMPONE from the maximum current values measured at different scan rates. Calculation of D requires knowledge of the concentration of TEMPONE in the swollen polymer network. In fact, while our experiments were carried out by using DMF solutions containing 10^{-2} M TEMPONE, the solute concentration in gels may be defined as either the amount of solute per unit volume of the swelling medium in the gel (i.e., the same C value as in bulk DMF) or the amount of solute per unit volume of gel (C').[28] C' can be calculated from C using $C'=(1-\varphi)C$. The D values calculated by either assumption are shown in Table 3. The results obtained by the two methods showed that the diffusion of TEMPONE was reduced very markedly by an increase of the degree of polymer cross-linking. To investigate possible effects of the supporting electrolyte on the diffusion of TEMPONE, we carried out a few experiments either with a lower TEAP concentration or with 0.6 M $LiClO_4$. These results, which are also included in Table 3, evidence a significant effect of the concentration and/or the nature of the electrolyte on D.

Table 3. Diffusion coefficients of TEMPONE in DMF and swollen CFPs **M1**–**M5**, as determined from CV experiments at 22 °C.

Medium	D [10^{-7} cm^2s^{-1}][a]					
	DMF/0.6 M TEAP		DMF/0.2 M TEAP		DMF/0.6 M $LiClO_4$	
Bulk	60(3)		74(4)		77(2)	
M1	18.8(2.9)	22.6(3.4)				
M2	6.8(1.3)	10.2(1.8)	13.8(2.8)	19.4(3.9)	12.6(2.4)	19.2(4.4)
M3	4.1(1.0)	6.4(1.5)				
M4	2.7(1.3)	4.8(2.1)				
M5	1.0(0.2)	2.8(0.5)	2.5(0.5)	6.1(1)		

[a] The second value refers to the D value calculated with Equation (7) using C'. The experimental uncertainty is provided in parentheses.

$$i = 4nFDCr[0.34\exp(-0.66p) + 0.66 - 0.13\exp(-11/p) + 0.351p] \quad (7)$$

Besides physical diffusion, the redox couple may also be transported by electron-hopping (self-exchange) between the oxidized and reduced forms of the electroactive species. This mechanism may enhance the observed diffusion coefficient (D_{obsd}) according to the Dahms–Ruff equation[34] [Eq. (8), where k_{ex} is the electron self-exchange rate constant at the center-to-center distance d]. The effect of the self-exchange reaction is particularly important for species characterized by very small D values and reorganization energies (and thus large k_{ex} values). In general, although D values in solution commonly lie in the range of 10^{-6}–10^{-5} cm^2s^{-1}, and thus the effect of the self-exchange contribution is negligible, the situation may be different in more viscous media.[35] We took this factor into account. A k_{ex} value of 2×10^8 $M^{-1}s^{-1}$ has been reported for the $TEMPO^+$/TEMPO couple (TEMPO = 2,2,6,6-tetramethyl-1-piperidinyloxyl radical) in aprotic organic solvents.[36] Since the two radicals are similar, we used the latter value of k_{ex} for TEMPONE. The D values obtained in the DMF solutions were used to estimate the D value at zero electrolyte concentration, taking advantage of the fact that the drop of D with electrolyte concentration in organic solvents is satisfactorily linear.[21] Then, by using Equation (6), we calculated $r=$ 3.4 Å and hence $d=6.8$ Å. This r value is identical to the value calculated by using the van der Waals volume of TEMPONE. By using this procedure we obtained a value of 1.6×10^{-9} cm^2s^{-1} for the second term of the right-hand side of Equation (8). Because this contribution is approximately two orders of magnitude smaller than the smallest of our experimental D values, it follows that our results refer only to physical diffusion, even for diffusion in swollen **M5**.

$$D_{obsd} = D + \frac{k_{ex}d^2C}{6} \quad (8)$$

The effect of φ on the diffusion coefficient of TEMPONE was also examined in DMF/0.6 M TEAP solutions of non-cross-linked PVP. The φ values were calculated from the polymer mass concentration w and the density data, assuming volume additivity. The results are presented in Table 4 and show a decrease of D with increasing φ. This decrease, however, is less marked than in **M1**–**M5**. This comparison indicates that beside the value of φ the cross-linking degree also has a very important effect on the value of D.

Analysis of the diffusivity data: In agreement with previous findings,[12b,13] $\ln\tau$ depends linearly on φ (Figure 4) in bulk DMF through to **M4**. This trend is as predicted from classic hydrodynamics (Stokes–Einstein rotational diffusion) on the basis of the Nicodemo–Nicolais relationship, $\eta=\eta_0\exp(-\nu\varphi)$ (where η_0 is the viscosity of the pure solvent and ν is an ad-

Table 4. Diffusion coefficients of TEMPONE dissolved in DMF/0.6 M TEAP solutions of non-cross-linked PVP at 22 °C.

wt %	φ	$D(\pm 4\,\%)$ [10^{-7} cm^2 s^{-1}]
0	0	60.0
7	0.054	49.0
8	0.061	47.6
9	0.069	45.6
10.5	0.081	43.7
11.9	0.092	41.1
17.8	0.140	31.3
22.3	0.178	26.7
24.6	0.197	20.2
29.6	0.240	15.5
34.5	0.284	9.6

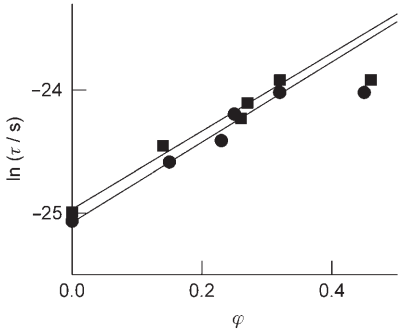

Figure 4. Dependence of the rotational correlation time τ of TEMPONE, dissolved in DMF (●) or DMF/0.6 M TEAP (■) confined inside CFPs **M1**–**M5**, on polymer volume fraction φ. The solid lines are the best linear fits to the data up to **M4**.

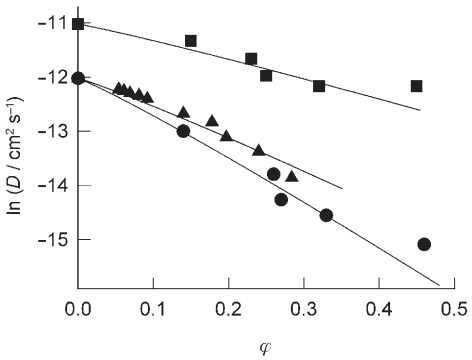

Figure 5. Dependence of the diffusion coefficient of DMF and TEMPONE in either swollen CFPs **M1**–**M5** or in PVP solutions on the polymer volume fraction φ: (■) DMF in CFPs **M1**–**M5**; (●) TEMPONE in CFPs **M1**–**M5** swollen with DMF/0.6 M TEAP; (▲) TEMPONE in solutions of PVP in DMF/0.6 M TEAP. The D values of TEMPONE were calculated from Equation (7) using C'. The lines are the best fits to the data (**M5** not included) obtained using Equation (9), as explained in the text.

justable parameter) that refers to the viscosity of concentrated suspensions of fibers.[37] As indicated by the slightly larger values of τ determined for the DMF/TEAP swollen CFPs, TEAP (0.6 M) caused a moderate increase in the microviscosity relative to bulk DMF.

Figure 5 shows that approximately linear dependences of $\ln D$ on φ hold for CFPs **M1**–**M4** and the non-cross-linked PVP solutions. Consistent with the ESR spectroscopy observations, the diffusion coefficients measured for TEMPONE and DMF inside swollen **M5** are slightly larger than the values expected from the trends displayed by the **M1–M4** data. Figure 5 illustrates that the diffusion coefficients of TEMPONE in the PVP solutions and in the swollen CFPs are significantly smaller than those observed in bulk DMF. In addition, the decrease in TEMPONE mobility inside the polymer networks is appreciably larger than that found for the DMF solvent molecule in the same swollen CFPs: for example, whereas in **M4** the relative decrease (D/D_0, where D_0 is the value in DMF) of the diffusion of TEMPONE is 0.08, the corresponding value for DMF is 0.32. In fact, DMF has a smaller radius than TEMPONE (see below) and this not only affects the absolute D values of the two species, but it is also expected to make their dependence on the cross-linking degree quite different. As a matter of fact, it has been shown that under otherwise identical experimental conditions (polyelectrolyte solution) ultramicroelectrode CV and PGSE-NMR spectroscopy provide D values that are in good agreement.[38]

The presence of an electrolyte did not affect the swelling behavior but increased the solution viscosity. Table 2 shows that the rotational correlation time of TEMPONE increased when TEAP was added to the solution, which indicates that to some extent the rotational mobility was hampered. Similarly, the presence of an electrolyte such as $LiClO_4$ caused the self-diffusion coefficient of DMF to decrease in both the bulk solvent and swollen **M2** (Table 2). Although the diffusion coefficient of TEMPONE had to be measured by CV in DMF containing a background electrolyte, an important effect of the latter on D was evidenced by experiments performed either with a different electrolyte or by changing its concentration (Table 3). In particular, when the swelling medium was changed from DMF/0.6 M TEAP to DMF/0.2 M TEAP a remarkable increase of D for TEMPONE was observed in the bulk solution and the polymer networks of swollen **M2** and **M5**.

A viscosity dependence of electrolyte solutions on the electrolyte concentration is documented in the literature.[39] In particular, the viscosity of amide solvents containing quaternary ammonium halides was reported to be significantly influenced by a variation of the electrolyte concentration.[40] Thus, the higher D values observed for DMF compared with those determined for TEMPONE are related to both a smaller radius and a higher viscosity of DMF/0.6 M TEAP compared with DMF. On the other hand, the greater sensitivity of TEMPONE diffusion on the cross-linking degree cannot be explained in terms of the Nicodemo–Nicolais relationship, which does not take into account any dependence of diffusion on the dimensions of either the diffusing molecule or the polymer fibers. More complex diffusion models[41] based on the obstruction concept and sometimes including hydrodynamic effects need to be considered to better rationalize the observed behavior.

Another important observation stemming from the data in Figure 5 is that for any given φ value the D values obtained for TEMPONE in DMF solutions of PVP are consistently larger than those measured in the swollen CFPs. According to literature data, the effect of cross-linking on the translational mobility of molecules in swollen CFPs is not quite clear. Gao et al. found that the diffusion coefficient of perdeuteriated TEMPONE, as measured by ESR spectroscopic imaging, is smaller in cross-linked polystyrene networks swollen by toluene than the value determined in polystyrene/toluene solutions with the same polymer content.[42] Johansson et al. also observed that the translational diffusion of poly(ethylene glycols) is faster in solutions of flexible polymers than in solutions containing rigid ones.[43] On the other hand, Pickup et al.[44] observed similar D values for toluene confined inside the gel domains of cross-linked polystyrene and toluene solutions containing non-cross-linked polystyrene but characterized by identical φ values.

Beside the viscosity increase caused by the confinement of the solution inside the polymer network, a polymer also causes an increase of the average path length available for diffusion. In essence, the permeability of the polymer to different molecules is expected to be related to both their dimensions and the stiffness and molecular size of the polymer network chains. Several models have been proposed to describe the diffusivity of solutes within gels, as comprehensively reviewed by Amdsen.[41] Whereas some of them cannot be employed to fit our data as their applicability is more appropriate to describe the diffusion of large molecules, such as models combining hydrodynamic and obstruction effects, others rely on undefined parameters. Finally, some models display curvatures in the $\ln D$ versus φ plots that are opposite to what was actually observed for the investigated systems (cf. Figure 5). We applied the obstruction model developed by Johansson and Löfroth as it relies on simple parameters and is appropriate for solutes with $r <$ 30 Å.[45] According to this model, which is based on the Ogston concept of the distribution of space in a suspension of fibers,[46] the diffusion coefficient of a solute (assumed to be a hard sphere of radius r) inside a rigid polymer network of fibers with radius r_f is related to the diffusion coefficient in the pure solvent (D_0) by the stretched exponential given in Equation (9), where $\alpha = \varphi[(r+r_f)/r_f]^2$. Whereas the value of r for TEMPONE was determined by CV to be 3.4 Å, in excellent agreement with molecular models, the r value for DMF cannot be calculated from the experimental data by using the Stokes–Einstein equation as DMF is the solvent itself. Its radius was calculated from the r value for TEMPONE and the D values of both TEMPONE and DMF in the same medium (DMF/0.6 M $LiClO_4$) using equation $r_{DMF} = (D_{TEMPONE} \times r_{TEMPONE})/D_{DMF}$. The resulting value, 2.3 Å, is identical to that obtained from molecular models. Estimating the value of r_f, however, is less straightforward as the PVP chains have an uneven section approximately in the range of 2–3 Å. However, because of the various assumptions of the model, which forcefully uses an idealized picture of the polymer network, we decided to estimate r_f empirically by applying Equation (9) to the PVP data (Figure 5) and imposing the above r value for TEMPONE. The resulting r_f value, 2.2 Å, may appear a bit small, but, on the other hand, it should be considered more as an effective fiber radius rather than a dimension with a precise physical meaning. It is also worth mentioning that Equation (9) was also adapted[45] to the case of worm-like polymers by defining α as $\alpha = \varphi[(r+r_f)/r_f]^v$, where the scaling parameter v may range from 1 to 2 and decreases as the flexibility increases. However, fitting the experimental data with $v < 2$ led to smaller r_f values, and thus we preferred to carry on using the original $v = 2$ value.

$$D = D_0 \exp(-0.84\alpha^{1.09}) \quad (9)$$

The fits to the experimental data obtained for DMF and TEMPONE in the swollen CFPs are also shown in Figure 5. The calculated DMF and TEMPONE radii, obtained by using Equation (9) and $r_f = 2.2$ Å, are 2.2 and 4.2 Å, respectively (for reasons already discussed, we did not include the **M5** data in the fitting procedure; their inclusion, however, led to the slightly smaller values of 1.9 and 4.0 Å). Although the DMF radius is in good agreement with the expected value, the apparent r of TEMPONE in the swollen CFPs is substantially larger than its hydrodynamic radius. Overall, these findings indicate that for the small solutes (and relatively large φ values) characterizing our study, the obstruction model of Johansson and Löfroth satisfactorily describes the diffusivity in the polymer networks investigated. Whereas a good agreement between theory and experimental data has been verified for the small DMF molecule, the larger TEMPONE probe behaved in the cross-linked CFPs as if it had a larger size. The presence of an electrolyte in the determinations of TEMPONE diffusion is also expected to play a role by increasing the solution viscosity. However, the fact that the estimated r_f value satisfactorily accounts for both the TEMPONE data in the PVP solutions (carried out in the presence of 0.6 M TEAP) and the data for DMF in the swollen CFPs (no electrolyte) would suggest that the decrease in D for a larger molecule induced by an increase in electrolyte viscosity is to some extent matched by the effect on the diffusion of a smaller probe caused by cross-linking. On the other hand, the results obtained with TEMPONE in the two types of media (both in the presence of 0.6 M TEAP) indicate that the calculated apparent increase in the radius of TEMPONE in the swollen CFPs reflects, in fact, an increase in the diffusion path length through the polymer pores, also relative to the diffusivity of the small DMF molecule in the same media.

Conclusion

ESR spectroscopy, PGSE-NMR spectroscopy, and ultramicroelectrode CV have been successfully employed to obtain a consistent picture of the diffusivity of molecular probes inside polymer frameworks swollen by DMF. The rotational

mobility of TEMPONE and the translational mobility of the same probe and the swelling medium correlate well with the CFP volume fraction, φ. The diffusion of TEMPONE is substantially more sensitive to φ variations than that of DMF, which is partially accounted for by the difference in size of the two probes. TEMPONE diffusion in the swollen polymer framework is more dependent on φ than in solutions of non-cross-linked PVP. Application of the model developed by Johansson and Löfroth points to an apparent increase of the TEMPONE hydrodynamic radius in the more structured media, which translates into an increase of the diffusion path length. These findings show that useful and convergent information can be obtained by a combined ESR spectroscopy, PGSE-NMR spectroscopy, and ultramicroelectrode CV approach. They also agree with previous results, obtained with other swollen materials, on the correlations between rotational and translational mobilities and the polymer-chain concentration.[12,13]

Acknowledgements

This work was financially supported by the Ministero dell'Istruzione, dell'Università e della Ricerca (MIUR).

[1] A. Guyot in *Synthesis and Separations Using Functional Polymers* (Eds.: D. C. Sherrington, P. Hodge), Wiley, New York, **1988**, pp. 1–42.
[2] *Ion-Exchangers* (Ed.: K. Dorfner), Walter de Gruyter, Berlin, **1991**; C. E. Harland, *Ion Exchange*, Royal Society of Chemistry, Cambridge, **1994**.
[3] M. A. Harmer, Q. Sun, *Appl. Catal. A* **2001**, *221*, 45–62.
[4] J. S. Früchtel, G. Jung, *Angew. Chem.* **1996**, *108*, 19–46; *Angew. Chem. Int. Ed. Engl.* **1996**, *35*, 17–42.
[5] a) W. O. Haag, D. D. Whitehurst (Mobil Oil), German Patent 1800379, **1969**; [*Chem. Abstr.* **1970**, *72*, 31192]; b) W. O. Haag, D. D. Whitehurst (Mobil Oil), German Patent 1800371, **1969**; [*Chem. Abstr.* **1969**, *71*, 114951]; c) W. O. Haag, D. D. Whitehurst (Mobil Oil), German Patent 1800380, **1969**; [*Chem. Abstr.* **1969**, *71*, 33823].
[6] R. H. Grubbs, *CHEMTECH* **1977**, *7*, 512–518.
[7] B. Corain, P. Centomo, M. Zecca, *Chim. Ind. (Milan, Italy)* **2004**, *86*, 114–121, and references therein.
[8] For example, see: F. R. Hartley, *Supported Metal Complexes*, Reidel, Dordrecht, **1985**.
[9] N. Yoneda, S. Kusano, M. Yasui, P. Pujado, S. Wilcher, *Appl. Catal. A* **2001**, *221*, 253–265.
[10] For example, see: a) C. Burato, P. Centomo, G. Pace, M. Favaro, L. Prati, B. Corain, *J. Mol. Catal. A* **2005**, *238*, 26–34; b) B. Corain, K. Jeøàbek, P. Centomo, P. Canton, *Angew. Chem.* **2004**, *116*, 977–980; *Angew. Chem. Int. Ed.* **2004**, *43*, 959–962; c) B. Corain, P. Centomo, S. Lora, M. Kralik, *J. Mol. Catal. A* **2003**, *204–205*, 755–762.
[11] For example, see: a) C. K. Y. Lee, A. B. Holmes, S. V. Ley, I. F. McConvey, B. Al-Duhri, G. A. Leeke, R. C. D. Santos, J. P. K. Seville, *Chem. Commun.* **2005**, 2175–2177; b) Y. Uozumi, R. Nakao, *Angew. Chem.* **2003**, *115*, 204–207; *Angew. Chem. Int. Ed.* **2003**, *42*, 194–197; c) F. Shi, Y. Deng, *J. Catal.* **2002**, *211*, 548–551.
[12] a) K. Jeøàbek in *Cross Evaluation of Strategies in Size-Exclusion Chromatography* (Eds.: M. Potschka, P. L. Dubin), ACS Symposium Series 635, American Chemical Society, Washington DC, **1996**, pp. 211–224; b) A. Biffis, B. Corain, M. Zecca, C. Corvaja, K. Jeøàbek, *J. Am. Chem. Soc.* **1995**, *117*, 1603–1606; c) K. Jeøàbek, *Anal. Chem.* **1985**, *57*, 1598–1602.
[13] A. A. D'Archivio, L. Galantini, A. Panatta, E. Tettamanti, B. Corain, *J. Phys. Chem. B* **1998**, *102*, 6774–6779.
[14] F. Pozzar, A. Sassi, G. Pace, S. Lora, A. A. D'Archivio, K. Jeøàbek, A. Grassi, B. Corain, *Chem. Eur. J.* **2005**, *11*, 7395–7404.
[15] P. Hodge, *Chem. Soc. Rev.* **1997**, *26*, 417–424.
[16] A. Biffis, R. Ricoveri, S. Campestrini, M. Kralik, K. Jeøàbek, B. Corain, *Chem. Eur. J.* **2002**, *8*, 2962–2967.
[17] F. Maran, unpublished results.
[18] a) H. Zhou, N. Gu, S. Dong, *J. Electroanal. Chem.* **1998**, *441*, 153–160; b) S. Dong, N. Gu, H. Zhou, *J. Electroanal. Chem.* **1998**, *441*, 95–101; c) M. Ciszkowska, J. G. Osteryoung, *J. Phys. Chem. B* **1998**, *102*, 291–297; d) O. Haas, C. S. Velázquez, Z. Porat, R. W. Murray, *J. Phys. Chem.* **1995**, *99*, 15279–15284; e) T. T. Wooster, M. L. Longmire, H. Zhang, M. Watanabe, R. W. Murray, *Anal. Chem.* **1992**, *64*, 1132–1140; f) M. Watanabe, M. L. Longmire, R. W. Murray, *J. Phys. Chem.* **1990**, *94*, 2614–2619; g) M. L. Longmire, M. Watanabe, H. Zhang, T. T. Wooster, R. W. Murray, *Anal. Chem.* **1990**, *62*, 747–752; h) L. Geng, R. A. Reed, M.-H. Kim, T. T. Wooster, B. N. Oliver, J. Egekeze, R. T. Kennedy, J. W. Jorgenson, J. F. Parcher, R. W. Murray, *J. Am. Chem. Soc.* **1989**, *111*, 1614–1619.
[19] a) M. Ciszkowska, M. D. Guillaume, *J. Phys. Chem. A* **1999**, *103*, 607–613; b) M. V. Mirkin, F. F. Fan, A. J. Bard, *Science* **1992**, *257*, 364–366.
[20] a) M. Opallo, J. Kukulka-Walkiewicz, M. Saczek-Maj, *J. Sol-Gel Sci. Technol.* **2003**, *26*, 1045–1048; b) M. M. Collinson, B. Novak, *J. Sol-Gel Sci. Technol.* **2002**, *23*, 215–220; c) A. R. Howells, P. J. Zambrano, M. M. Collinson, *Anal. Chem.* **2000**, *72*, 5265–5271; d) M. M. Collinson, P. J. Zambrano, H. Wang, J. S. Taussig, *Langmuir* **1999**, *15*, 662–668.
[21] F. Maran, M. S. Workentin, unpublished results.
[22] P. L. Nordio in *Spin Labeling, Theory and Applications* (Ed.: L. J. Berliner), Academic Press, New York, **1976**, pp. 5–52.
[23] M. F. Ottaviani, *J. Phys. Chem.* **1987**, *91*, 779–784; B. D. Chestnut, J. F. Hower, *J. Phys. Chem.* **1971**, *75*, 907–912.
[24] M. Brustolon, A. L. Maniero, C. Corvaja, *Mol. Phys.* **1984**, *51*, 1269–1281.
[25] P. T. Callaghan, *Principles of Nuclear Magnetic Resonance Microscopy*, Oxford University Press, New York, **1991**.
[26] J. Calfors, R. Rymden, *Eur. Polym. J.* **1982**, *18*, 933–937.
[27] B. R. Knauer, J. J. Napier, *J. Am. Chem. Soc.* **1976**, *98*, 4395–4400.
[28] A. H. Muhr, J. M. V. Blanshard, *Polymer* **1982**, *23*, 1012–1026.
[29] S. Pickup, F. D. Blum, *Macromolecules* **1989**, *22*, 3961–3968.
[30] G. Hradetzky, I. Hammerl, H.-J. Bittrich, K. Wehner, W. Kisan, *Selective Solvents*, Elsevier, Amsterdam, **1989**.
[31] The term "nanoporous" is utilized in accord with: *Handbook of Porous Solids* (Eds.: F. Schüth, K. Sing, J. Weitkamp), Wiley-VCH, Weinheim, **2002**.
[32] R. M. Wightman, D. O. Wipf in *Electroanalytical Chemistry, Vol. 15* (Ed.: A. J. Bard), Marcel Dekker, New York, **1989**, pp. 267–353.
[33] K. Aoki, K. Akimoto, K. Tokuda, H. Matsuda, J. Osteryoung, *J. Electroanal. Chem. Interfacial Electrochem.* **1984**, *171*, 219–230.
[34] a) M. Majda in *Molecular Design of Electrode Surface*s (Ed.: R. W. Murray), Wiley, New York, **1992**, pp. 159–206; b) I. Ruff, L. Botar, *J. Chem. Phys.* **1985**, *83*, 1292–1297; c) H. Dahms, *J. Phys. Chem.* **1968**, *72*, 362–364.
[35] A. M. Leone, S. C. Weatherly, M. E. Williams, H. H. Thorp, R. W. Murray, *J. Am. Chem. Soc.* **2001**, *123*, 218–222.
[36] G. Grampp, K. Rasmussen, *Phys. Chem. Chem. Phys.* **2002**, *4*, 5546–5549.
[37] L. Nicodemo, L. Nicolais, *Polymer* **1974**, *15*, 589–592.
[38] M. Ciszkowska, L. Zeng, E. O. Stejskal, J. G. Osteryoung, *J. Phys. Chem.* **1995**, *99*, 11764–11769.
[39] a) G. J. Janz, R. P. T. Tomkins, *Nonaqueous Electrolytes Handbook, Vol. I*, Academic Press, New York, **1972**; b) R. A. Robinson, R. H. Stokes, *Electrolyte Solutions*, Butterworths, London, **1959**, pp. 303–307.
[40] a) P. Haldar, D. K. Majumdar, *Z. Phys. Chem. (Muenchen Ger.)* **1990**, *167*, 69–80; b) M. Della Monica, S. Bufo, *Electrochim. Acta* **1977**, *22*, 1213–1218.

[41] B. Amsden, *Macromolecules* **1998**, *31*, 8382–8395.
[42] Z. Gao, J. Pilaø, S. Schlick, *J. Phys. Chem.* **1996**, *100*, 8430–8435.
[43] L. Johansson, C. Elvingson, J.-E. Löfroth, *Macromolecules* **1991**, *24*, 6024–6029.
[44] S. Pickup, F. D. Blum, W. T. Ford, M. Periyasami, *J. Am. Chem. Soc.* **1986**, *108*, 3987–3990.
[45] L. Johansson, J.-E. Löfroth, *J. Chem. Phys.* **1993**, *98*, 7471–7479.
[46] G. Ogston, *Trans. Faraday Soc.* **1958**, *54*, 1754–1757.

Received: September 5, 2006
Published online: December 14, 2006

